

CHAPTER 2

THEORY

In the analysis of flexibility of ninety degree single mitered pipe bends, we first determined them as a kind of lobster back bend but not smooth as the lobster bend. Lane and Rose⁽¹⁵⁾ found that by assuming that the lobster-back bend was replaced by a smooth bend of the same equivalent radius R , flexibility factors are obtained from Gross and Ford⁽⁹⁾ expression for overall deflection of a smooth bend fitted with equal tangent pipes

$$Y = \frac{F}{12E} \left[\frac{4C^3}{I} + \frac{KR}{I} \left\{ 3\pi C^2 + 6CR(4-\pi) + 6R^2(\pi-3) \right\} \right] \quad (1)$$

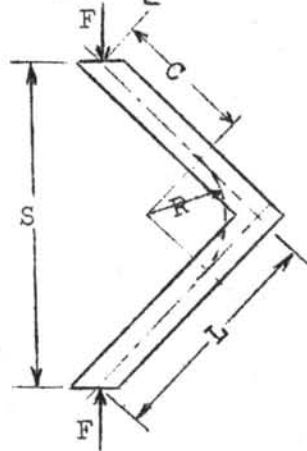


Fig 2-1. MITERED PIPE BEND AND
EQUIVALENT SMOOTH BEND.

The flexibility factors obtained are then compared with the values from the three terms, third approximation of Von Karman's analysis for equivalent smooth bend

$$K = \frac{252 + 73912\lambda^2 + 2446176\lambda^2 + 2822400\lambda^6}{3 + 3280\lambda^2 + 329376\lambda^4 + 2822400\lambda^6} \quad (2)$$

where λ is the pipe factor = $\frac{tR}{r^2}$

From the comparison it is seen that flexibility of lobster-back bend varied between 75-85% of the smooth bend value. Since the ninety degree single mitered pipe bend is not as smooth as the lobster back bend, we must find out at what equivalent radius R the flexibility factor from Gross and Ford expression will agree with that from the third approximation of Von Karman's analysis. These will indicate that at what equivalent radius will the smooth bend correspond to ninety degree single mitered bend.

In the analysis of stress around ninety degree mitered pipe bend we made the first assumption that the angle between pipe legs was always ninety degrees. The pipe that had no internal pressure was taken as the cantilever beam which was subjected to bending and axial compression by forces or moments applied at the free ends in the plane of the bend. Only the stresses at the same circular cross-section on the outer surface of the pipe would be determined and analysed. The second assumption was that the pipe material was isotropic material which was the material that had the same properties in all directions. The longitudinal stresses, S_z from experimental method by the use of strain-gage technique and Hooke's law for isotropic material⁽¹⁹⁾ were compared with the values from combined stress theory due to bending and axial compression. To make it easy and simple for this theory, it was assumed that the pipe was not warp or distorted, circular cross-sections remain circular after loaded.

The stress, S_z due to bending moment, M and the compressive force in an axial direction, F_z could be calculated from :

$$S_z = \frac{-F_z}{A} + \frac{My}{I}$$

where positive and negative signs expressed for tension and compression respectively.

$$\begin{aligned} S_z &= \frac{-F_z}{2\pi r t} + \frac{F_y x r \cos \alpha}{\pi r^3 t} \\ &= \frac{F}{2\pi r^2 t} [2x \sin \beta \cos \alpha - r \cos \beta] \end{aligned}$$

In this experiment $\beta = 45$ degrees, so that

$$S_z = \frac{F}{2\sqrt{2}\pi r^2 t} (2x \cos \alpha - r) \quad (3)$$

From the experimental study, by the use of strain gages and strain-gage technique as will be described in appendix I, the values of strain in longitudinal, e_z and circumferential, e_θ directions could be determined. By assuming that net strain in radial direction, e_r was zero, the stresses in longitudinal, S_z , circumferential, S_θ and radial, S_r directions could be determined from Hooke's law for an isotropic material⁽¹⁹⁾ as follows:

$$S_z = \frac{E}{1+\mu} \left[e_z + \frac{\mu}{1-2\mu} (e_z + e_\theta + e_r) \right], \quad S_{z\theta} = G e_{z\theta} \quad (4)$$

$$S_\theta = \frac{E}{1+\mu} \left[e_\theta + \frac{\mu}{1-2\mu} (e_z + e_\theta + e_r) \right], \quad S_{\theta r} = G e_{\theta r} \quad (5)$$

$$S_r = \frac{E}{1+\mu} \left[e_r + \frac{\mu}{1-2\mu} (e_z + e_\theta + e_r) \right], \quad S_{rz} = G e_{rz} \quad (6)$$

To find S_{ze} we made an assumption that the pipe composed of infinite horizontal plane and shear strain, e_{ze} vary from the top to the bottom plane in the form of parabolic curve where $e_{ze} = 0$ at top and bottom plane (position ± 90) and maximum at the center (zero degree position) as shown in Fig. 2-2.

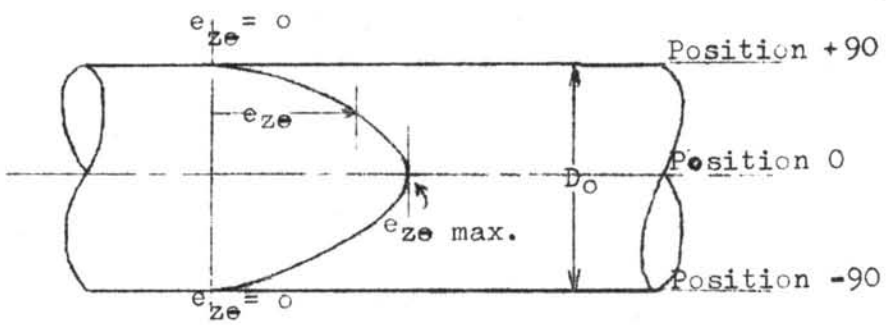


Fig. 2-2. VARIATION OF SHEAR STRAIN ON z-o PLANE



It is easily seen from Mohr's circle Fig. 2-3, that

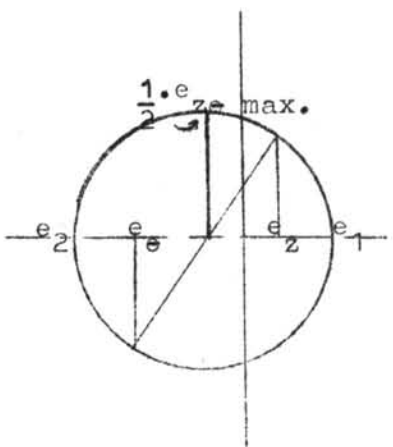


Fig. 2-3. MOHR'S CIRCLE.

$e_{ze \text{ max.}} = e_1 - e_2$ and we knew that at zero degree position maximum and minimum stress, strain made an angle 45 degrees with axial direction. So that if strain gages were attached on pipe wall at zero degree position and made an angle 45 degrees

with axial direction as shown in Fig. 2-4. e_1 and e_2 at each load would be measured, then $e_{ze \text{ max.}}$ at each load were obtained as shown in table 4-5. and e_{ze} at each point were

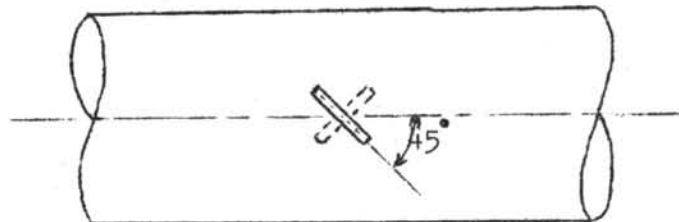


Fig. 2-4. POSITIONS OF STRAIN GAGES FOR THE MEASURING OF MAXIMUM AND MINIMUM STRAINS.

obtained too from the expression that was derived in appendix II, which showed that

$$e_{ze} = e_{ze \text{ max.}} \cos^2 \theta \quad (7)$$

then, S_{ze} could be found.

To make it easy to find S_{er} , it was assumed that these values equal to those of thin tubular cross-section. In Fig. 2-5., for uniform stress distribution across the thickness of the pipe wall, shear stress in e-r plane along section 1-1 could be expressed⁽²⁰⁾ by

$$S_{er} = \frac{Vr^2 \sin \alpha}{I}$$

where $I = \pi r^3 t$ for thin tubular pipe

$$V = F_y = F \sin \beta = \frac{F}{\sqrt{2}}$$

$$\text{so that } S_{er} = \frac{F \sin \alpha}{\sqrt{2} \pi r t} \quad (8)$$

For the known value of load F , radius r and thickness t of the pipe, shear stress S_{er} at the corresponding angle α can be determined.

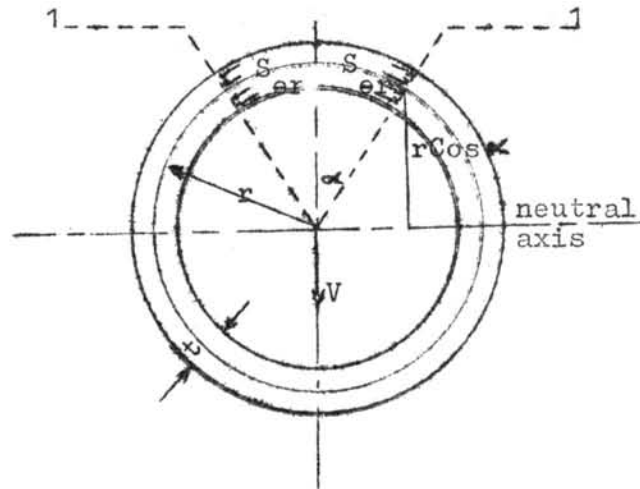


Fig. 2-5. VARIATION OF SHEAR STRESS ON $e-r$ PLANE.

The last term to determine was S_{rz} , this shear stress between adjacent fibers varies with the distance S as shown in Fig. 2-6., being maximum at the neutral plane and zero at each free edge. From the requirement for equality of complementary shear stress, we may now conclude that there must be the same shear stress distribution in the plane of the cross-section, so that S_{rz} could be determined.

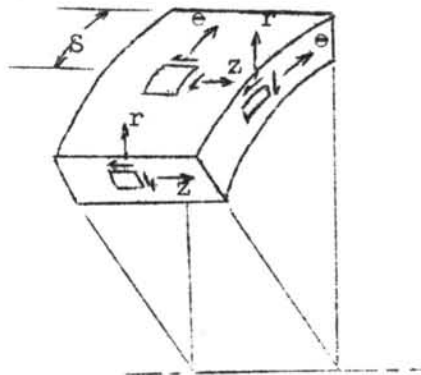


Fig. 2-6. SHEAR STRESSES IN EACH PLANE.